Korean J. Chem. Eng., **17**(1), 47-51 (2000)

Interpretation of Hydrothermal Crystallization of Fine $BaTiO_3$ Powders

Kyung Won Seo† and Jung Kang Oh

School of Chemical Engineering & Biotechnology, Ajou University, Suwon 440-749, Korea
(*Received 4 August 1999 • accepted 8 November 1999*)

Abstract–In the preparation of fine $BaTiO_3$ powders under hydrothermal conditions, the reaction mechanism was interpreted through solid-state kinetic analysis of the Johnson-Mehl-Avrami plot. In this experiment reactants were dissolved and consumed to spherical particles of 50 nms from aggregation of several nanometer-sized particles. The particulate formation of $BaTiO_3$ underwent a 1st-order hydrolysis-condensation reaction with phase-boundary transition in the early stage of the reaction regardless of the initial concentration of the feedstock. However, as the concentration of nutrients was reduced, dissolution followed by precipitation became dominant, and a diffusion-controlled reaction proceeded. When the concentration of nutrients was reduced to an extent that was not high enough to sustain supersaturation, the reaction was controlled by solidification for encapsulation of aggregated particles, inside of which the diffusion-controlled reaction slowly proceeded.

Key words: Hydrothermal, $BaTiO_3$, Johnson-Mehl-Avrami, Hydrolysis-condensation, Phase-boundary Transition, Dissolution, Precipitation, Supersaturation, Diffusion-controlled

INTRODUCTION

Particle synthesis through hydrothermal reaction has been recognized as a viable chemical process for production of wide varieties of commercially important advanced ceramic powders [Geiger, 1995]. The particles prepared by hydrothermal synthesis are very fine, not agglomerated, and good in crystallinity with narrow particle size distribution. Therefore, fine, highly purified, and homogeneous particles of multicomponent metal oxides can be produced through hydrothermal reactions under the appropriate conditions.

Previous reports on experimental results [Oh and Seo, 1999] show that $BaTiO_3$ particles seem to be prepared by hydrothermal crystallization through a multiple reaction procedure that includes dissolution, precipitation, hydrolysis-condensation, aggregation, diffusion and transformation, but not any single step controls the overall crystalline particle formation reaction. However, the basic reaction mechanism and kinetics of the hydrothermal particulate formation reaction have not correctly appeared yet due to experimental difficulties in data collection.

To analyze the kinetics of the dehydroxylation of kaolinite and of brucite and the decomposition of $BaCO_3$, Hancock and Sharp [1972] introduced a method of comparing the kinetics of isothermal solid-state reactions based on the classical equation suggested by Johnson, Mehl and Avrami for analysis of nucleation-and-growth process. Rossetti et al. [1992] applied this method to interpret the kinetics for the hydrothermal crystallization of $PbTiO_3$ powders.

The Johnson-Mehl-Avrami equation is known as:

$$f=1-\exp(-rt^m),$$

or, in linear form,

$$-\ln[\ln(1-f)]=\ln(r)+m\ln(t)$$

where

f: fractional yield of the crystallized particles at time t
r: a constant that partially depends on nucleation frequency and rate of grain growth
m: a constant that varies with the system geometry.

In accordance with the experimental results published by Hancock and Sharp [1972] for reactions obeying a single theoretical rate expression, Rossetti et al. [1992] reported that m has a value falling within a range characteristic of three distinct reaction mechanisms. For m=0.54-0.62, a diffusion-controlled process is dominant, while a first-order or phase-boundary controlled mechanism is indicated for m=1.0-1.24. A mechanism involving nucleation and growth control is shown when m=2.0-3.0. Values of m lying outside of the specified ranges have no obvious mechanistic interpretation, but can sometimes indicate competing processes. The various standard solid-state reaction rate equations and associated values of m are summarized in Table 1 [Hancock and Sharp, 1972; Rossetti et al., 1992].

Table 1. Solid-state reaction rate equation [Hancock and Sharp, 1972; Rossetti et al., 1992]

Function	Impilied mechanism	Equation	m
$D_1(f)$	Diffusion controlled	$f^2=kt$	0.62
$D_2(f)$	Diffusion controlled	$(1-f)\ln(1-f)+f=kt$	0.57
$D_3(f)$	Diffusion controlled	$[1-(1-f)^{1/3}]^2=kt$	0.54
$D_4(f)$	Diffusion controlled	$1-2f/3-(1-f)^{2/3}=kt$	0.57
$F_1(f)$	First order	$-\ln(1-f)=kt$	1.00
$R_2(f)$	Phase boundary	$1-(1-f)^{1/2}=kt$	1.11
$R_3(f)$	Phase boundary	$1-(1-f)^{1/3}=kt$	1.07
$Z_1(f)$	Zero order	$f=kt$	1.24
$A_2(f)$	Nucleation and growth	$[-\ln(1-f)^{1/2}]=kt$	2.00
$A_3(f)$	Nucleation and growth	$[-\ln(1-f)^{1/3}]=kt$	3.00

†To whom correspondence should be addressed.
E-mail: kwseoi@madang.aju.ac.kr

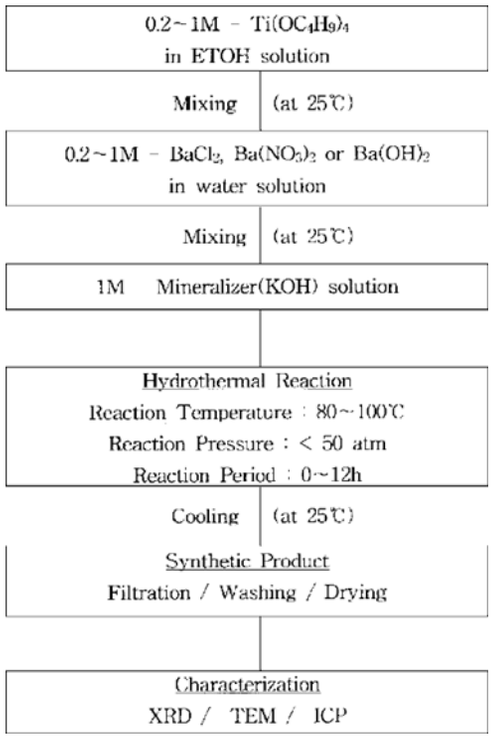

Fig. 1. Experimental procedure.

In this study, the experimental results on the hydrothermal crystallization of $BaTiO_3$ powders were obtained and interpreted through solid-state kinetic treatment of Hancock and Sharp [1972] for understanding the crystal formation mechanism.

EXPERIMENTAL PROCEDURE

The experimental procedures are schematically shown in Fig. 1. About 0.2 M to 1 M solution of each starting material was put into an autoclave with addition of mineralizer, 1 M-KOH. Mineralizer was added to increase solubility of the feedstock. The autoclave (Autoclave model HAST C-276, USA), which was used for hydrothermal reactions, had 1.0 liter of working volume and was made of hastelloy. The volume of the feedstock was kept constant throughout the whole experiments. The range of reaction temperature was 80 °C to 100 °C, and that of reaction time was 0 to 12 hrs. After the autoclave apparatus was cooled, the product was filtered, and then washed successively with deionized water to remove impurities. The synthetic product was then dried in a freezing dryer. The chemicals used in this work were of extra pure reagent grade.

The products were analyzed by an X-ray diffractometer (XRD: MXP3, Mac Science Co.) using a monochromatic CuK_α radiation, 40 kV, 20 mA, to determine the degree of the relative crystallinity of the product. The morphology of the product particles was observed by using a TEM (JEOL, EM-2000 EX II). The contents of Ba and Ti were measured by using a ICP (Perkin Elmer Optima 3000). In this paper, fractional yield (f) was defined as the molar ratio of $BaTiO_3$ crystals to Ti-compounds (includes $BaTiO_3$) in the synthetic powders, and calculated from ICP data.

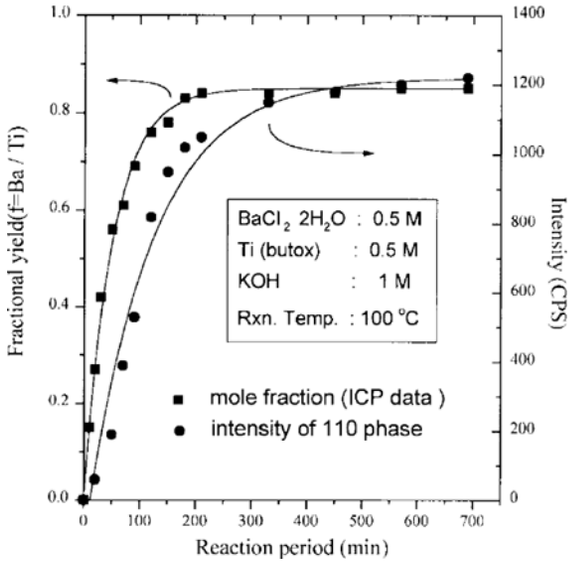

Fig. 2. Fractional yield and 110 face XRD intensity of product $BaTiO_3$ powders as a function of reaction period at 110 °C [with agitation (500 rpm), 0.5 M $BaCl_2 \cdot 2H_2O$, 0.5 M Ti (butox) and 1 M KOH].

RESULTS AND DISCUSSION

Fig. 2 shows the dependency of fractional yield (f=Ba/Ti) and (110) face XRD intensity of product powders on reaction-time when 0.5 M $BaCl_2 \cdot 2H_2O$, 0.5 M Ti(butox) and 1 M KOH were used, and the reaction temperature was 100 °C. As shown in this figure, the fractional yield and XRD intensity increased gradually up to 200 minutes past the beginning of the reaction. However, after 200 minutes elapsed, changes were not considerable due to the almost complete consumption of feedstock.

The fractional yield (f=Ba/Ti) data shown in Fig. 2 was rearranged by Johnson-Mehl-Avrami equation [Hancock and Sharp, 1972; Rossetti et al., 1992]. A plot of $\ln[-\ln(1-f)]$ against $\ln(t)$ over f=0.1-0.83 is shown in Fig. 3. A Johnson-Mehl-Avrami plot of the fractional yield (f) of $BaTiO_3$ crystals prepared at 80 °C with

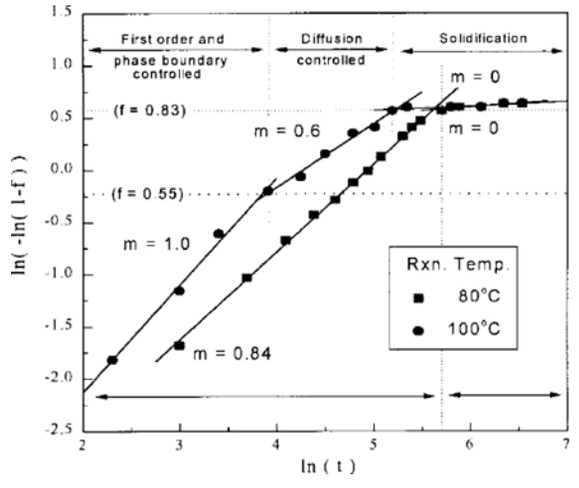

Fig. 3. Plots based on the Johnson-Mehl-Avrami analysis of the experimental data shown in Fig. 2; f=Ba/Ti, m=system geometry, t=time (min).

the same feedstock concentration is also shown in the figure. In the reaction at 100 °C, the geometric constant, m, is 1.0 till the fractional yield (f) gets to 0.55, and m is 0.6 when f is over 0.55 up to 0.83, and m is nearly zero when f is over 0.83. However, in the reaction at 80 °C, m is 0.84 when f is less than 0.83, and m is about zero when f is over 0.83. According to Hancock and Sharp [1972], and Rossetti et al. [1992], it can be said that in the reaction at 100 °C, the particulate formation reaction of $BaTiO_3$ crystals undergoes 1st-order hydrolysis-condensation after phase boundary transition when m is about 1.0, and that a diffusion-controlled process prevails when m is about 0.6. However, in the reaction at 80 °C, when m is 0.84, the particulate formation reaction is influenced by both of them, and dissolution followed by precipitation proceeds. The phase-boundary transition is not clearly shown in the figure. When m is about zero, solidification for encapsulation of aggregated particles is expected. Therefore, as the reaction temperature decreases, critical nuclei are produced relatively slowly due to the retardation of particulate formation reaction, and the nuclei generated earlier seem to undergo competitively hydrolysis-condensation and a diffusion-controlled step.

Fig. 4 shows the TEM micrographs of the synthetic powders prepared at 100 °C for different reaction periods, when 0.5 M $BaCl_2 \cdot 2H_2O$ and 0.5 M Ti(butox) of mixed solutions were used with 1 M KOH. Fig. 4(A) is for a 20 minutes' reaction, and the fractional yield was 0.27. Fig. 4(B) is for a 60 minute reaction, and the fractional yield was 0.55. The particles shown in this figure are seem to be crystal nuclei. In Fig. 4(C), we can see spherical particles of about 50 nms. Several nanometer-sized particles are aggregated inside of these particles. The reaction time was 160 minutes and the fractional yield was 0.79. Fig. 4(D) shows firmly solidified particles of about 30 nms, which were obtained from a 500 minute reaction. The fractional yield was 0.85. The XRD patterns of synthetic powders for these four cases are shown in Fig. 5. As shown in this figure, the particles shown in Fig. 4 (A) are amorphous, and those shown in other figures [from Figs. 4(B) to 4(D)] are crystals.

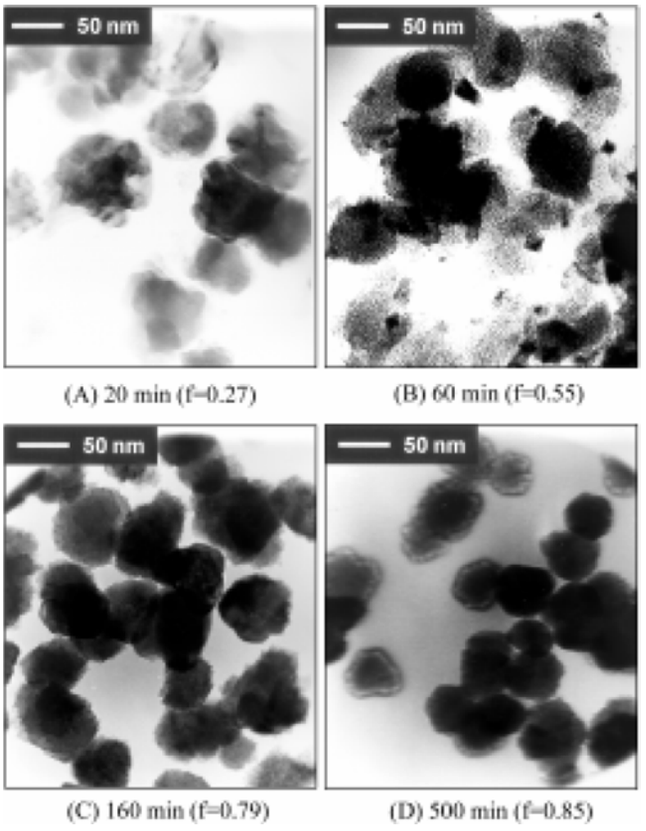

Fig. 4. TEM micrographs of hydrothermally prepared $BaTiO_3$ powder at 100 °C for different reaction periods [0.5 M $BaCl_2 \cdot 2H_2O$, 0.5 M Ti(butox) and 1 M KOH].

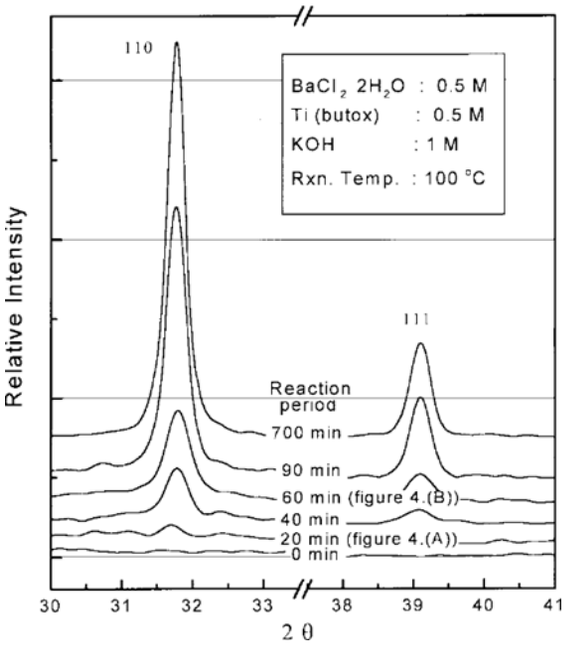

Fig. 5. XRD patterns of $BaTiO_3$ powder at 100 °C for different reaction periods [0.5 M $BaCl_2 \cdot 2H_2O$, 0.5 M Ti(butox) and 1 M KOH].

As mentioned in the previous works [Oh and Seo, 1999], hydrothermal synthesis of $BaTiO_3$ powder was expected to undergo multiple reaction steps that include dissolution, precipitation, hydrolysis-condensation, aggregation, internal diffusion and transformation. Therefore, as we see in these figures, $BaTiO_3$ particles were produced through 1st-order hydrolysis-condensation reaction when the fractional yield was less than 0.6, and through dissolution followed by precipitation before 0.83 of fractional yield was obtained. After that they underwent solidification for encapsulation of spherical surface, inside of which several nanometer-sized particles were aggregated and the diffusion-controlled reaction proceeded slowly.

Fig. 6 shows the variation of the fractional yield of $BaTiO_3$ as a function of the reaction period at different concentrations of feedstock (0.2-1.0 M) at 100 °C with a fixed value of $BaCl_2 \cdot 2H_2O$: Ti(butox) : KOH as 1 : 1 : 2. As shown in this figure, in the early stage of the reaction the rate of particulate formation reaction increased sharply until about 100 minutes passed when the feedstock concentration was less, equal to 0.6 M. However, the increase was not conspicuous after 100 minutes elapsed. When the feedstock concentration was higher, equal to 0.8 M, the reaction rate increased relatively slowly as the reaction time increased. In addition, the reaction rate decreased as the feedstock concentra-

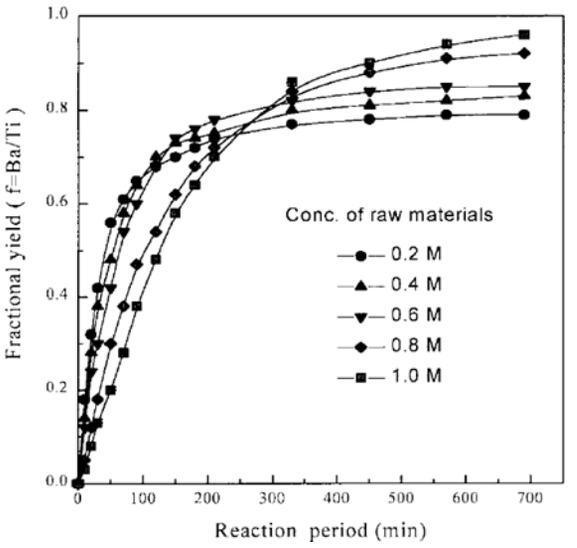

Fig. 6. Fractional yield of product $BaTi_5$ powder as a function of reaction period at 100 °C [with agitation (500 rpm), 0.5 M $BaCl_2 \cdot 2H_2O$, 0.5 M Ti(butox) and 1 M KOH].

tion increased in the early stage, while the fractional yield in the later stage increased. The above result is due to the following: In the early stage of the reaction the rate of consumption of feedstock becomes higher as the feedstock concentration decreases, since not only that the collision of barium cations with titanium cations carried by solvent occurs frequently, but that the dispersion of reacting particles is better. However, as the reaction proceeds the nutrients in the solution are sterilized, and the supersaturation is reduced; consequently, the particulate formation reaction slows down and is terminated finally.

When the feedstock concentration is low (<0.6 M), a part of the synthetic powders are reported to be amorphous because the level of supersaturation is low, unless the reaction time is prolonged sufficiently. However, as the concentration of feedstock

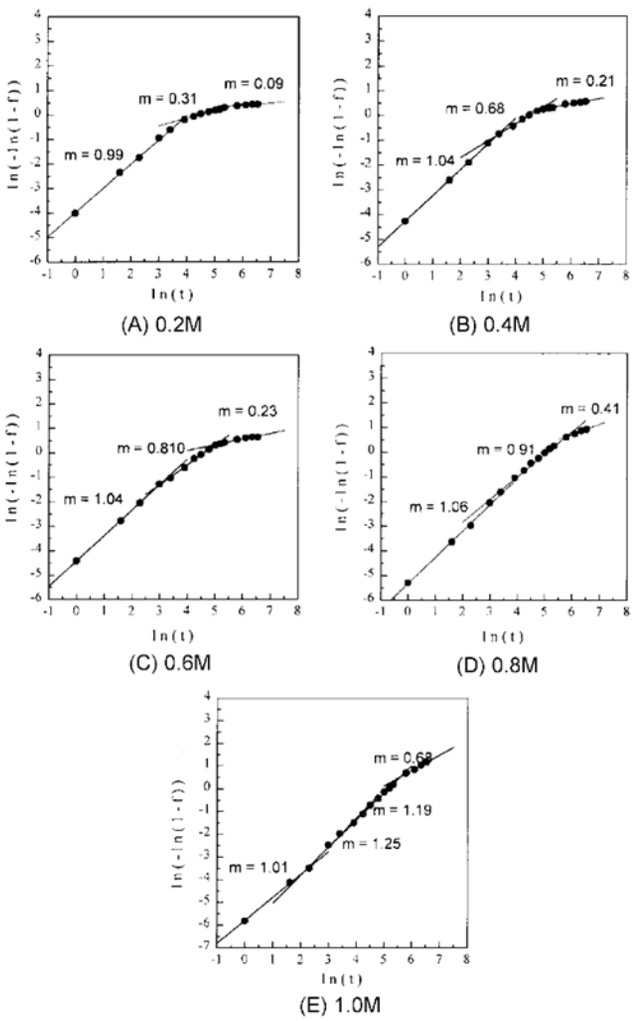

Fig. 7. Plots based on the Jonhson-Mehl-Avrami analysis of the experimental data shown in Fig. 6; f=Ba/Ti, m=system geometry, t=time (min).

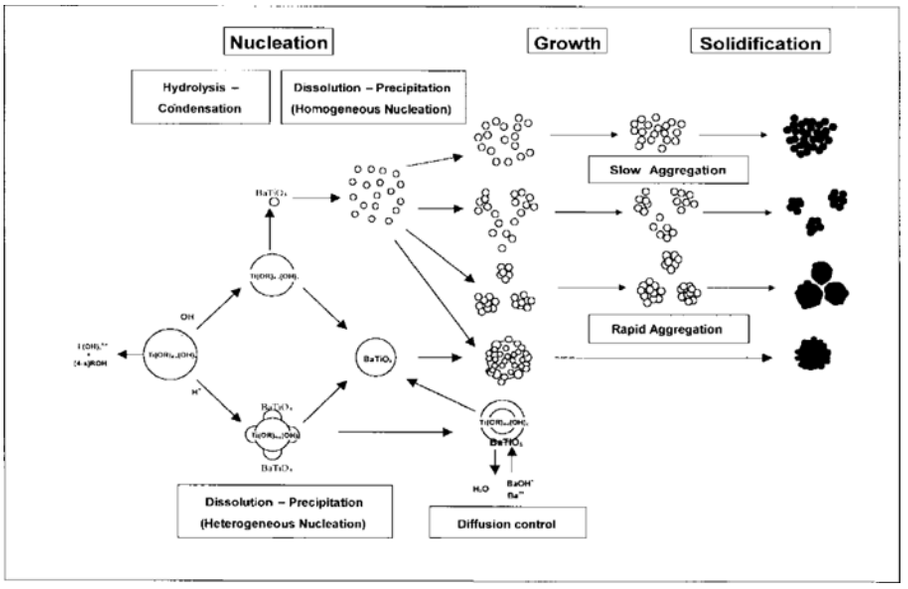

Fig. 8. Multiple reaction paths for hydrothermal crystallization of $BaTiO_3$ powders; includes hydrolysis-condensation, dissolution, precipitation, aggregation, diffusion and solidification [Oh and Seo, 1999].

increases, the supersaturation of the reactants increases, and consequently, most of the synthetic powders become crystals if the reaction proceeds over 60 minutes [Oh and Seo, 1999].

The fractional yields (f) shown in Fig. 6 are rearranged by the Johnson-Mehl-Avrami equation, and the results are shown in Fig. 7. This figure shows that in the early stage of the reaction, the geometric constant, m was about unity regardless of the initial concentration of the starting materials. However, as the reaction time elapsed, the value of m decreased. When the initial concentration of the feedstock was 0.2 M, the value of m at the end of the reaction was almost zero [Fig. 7(A)], but it was about 0.7 when the feedstock concentration increased to 1.0 M [Fig. 7(E)]. This means that the particulate formation undergoes various reaction steps depending upon the amount of nutrients left in the reacting solution. If the feedstock concentration increases further over 1.0 M, the value of m, throughout the entire range of reaction time, would be about unity, which suggests the crystallization mechanism as a 1st-order hydrolysis-condensation reaction.

From these results we can claim that the particulate formation reaction of $BaTiO_3$ undergoes 1st-order hydrolysis-condensation reaction with phase-boundary transition in the early stage regardless of the initial concentration of the feedstock, and that as the concentration of nutrients reduces along with the reaction proceeds, dissolution followed by precipitation becomes dominant, and a diffusion-controlled process proceeds. In addition, if the concentration of nutrients falls further to an extent that is not high enough to sustain supersaturation, solidification for encapsulation of the aggregated particles prevails, inside of which a diffusion-controlled reaction proceeds slowly. This claim was roughly predicted in the previous research work [Oh and Seo, 1999], and is schematically reformulated in Fig. 8.

CONCLUSION

Spherical particles of about 50 nms of $BaTiO_3$ powders were prepared by hydrothermal reaction, inside of which several nanometer-sized particles are aggregated. The crystal formation mechanism for this reaction was investigated through solid-state kinetic analysis of the Johnson-Mehl-Avrami equation. The results are summarized as follows:

1. As the reaction temperature decreased, critical nuclei were produced relatively slowly due to the retardation of particulate formation reaction.
2. In the early stage of the reaction the rate of particulate formation reaction decreased as the feedstock concentration increased, while the fractional yield in the later stage increased.
3. 1st-order hydrolysis-condensation with phase boundary transition was observed in the early stage of the reaction regardless of the initial concentration of the feedstock. However, as the concentration of nutrients was reduced, dissolution followed by precipitation became dominant, and a diffusion-controlled process proceeded.
4. When the concentration of nutrients fell further down to an extent that was not high enough to sustain supersaturation, the reaction was controlled by solidification for encapsulation of aggregated particles, inside of which the diffusion-controlled reaction slowly proceeded.

REFERENCES

Geiger, G., "Powder Synthesis and Shape Forming of Advanced Ceramics," *Am. Ceram. Soc. Bull.*, **8**(8), 62 (1995).

Hancock, J. D. and Sharp, J. H., "Method of Comparing Solid-State Kinetic Data and Its Application to the Decomposition of Kaolinite, Brucite, and $BaCO_3$," *J. Am. Ceram. Soc.*, **55**, 74 (1972).

Oh, J. K. and Seo, K. W., "Synthesis of Fine Powder for PTC-$BaTiO_3$," *HWAHAK KONGHAK*, **37**, 72 (1999).

Oh, J. K. and Seo, K. W., "Interpretation of Hydrothermal Synthesis of $BaTiO_3$ Powder," *Korean J. Ind. Eng. Chem.*, **10**, 509 (1999).

Rossetti, G. A., Watson, D. J., Newnham, R. E. and Adair, J. H., "Kinetics of the Hydrothermal Crystallization of the Perovskite $PbTiO_3$," *J. Cryst. Growth*, **116**, 251 (1992).